

Experimental study on characteristics of isopropanol ejection driven by electrohydrodynamics

Xi-Hao Zhang(张玺皓), Wen-Hua Wang (王文华), Cheng-Nan He(何承南), Yi-Chi Yao(姚奕弛), Bo-Yu Wang (王博宇), Xue-Hong Li(李学红), Zhi-Jian Wang(王智健), Chen Qiu(邱晨), Hai-Yi Sun(孙海轶), Yu-Xin Leng(冷雨欣), and Gang Xin(新刚)

Citation: Chin. Phys. B, 2025, 34 (**11**): 114701. DOI: 10.1088/1674-1056/addbcc
http://cpb.iphy.ac.cn; http://iopscience.iop.org/cpb

What follows is a list of articles you may be interested in

Nanobubbles produced by hydraulic air compression technique

Xiaodong Yang(杨晓东), Qingfeng Yang(杨庆峰), Limin Zhou(周利民),Lijuan Zhang(张立娟), and Jun Hu(胡钧)
Chin. Phys. B, 2022, 31 (**5**): 054702. DOI: 10.1088/1674-1056/ac464c

Crown evolution kinematics of a camellia oil droplet impacting on a liquid layer

Zhongyu Shi(石中玉), Guanqing Wang(王关晴), Xiangxiang Chen(陈翔翔), Lu Wang(王路), Ning Ding(丁宁), and Jiangrong Xu(徐江荣)
Chin. Phys. B, 2022, 31 (**5**): 054701. DOI: 10.1088/1674-1056/ac46c1

Droplets breakup via a splitting microchannel

Wei Gao(高崴), Cheng Yu(于程), Feng Yao(姚峰)
Chin. Phys. B, 2020, 29 (**5**): 054702. DOI: 10.1088/1674-1056/ab7b4b

Critical condition for the transformation from Taylor cone to cone-jet

Wei Cheng (魏承), Gang Tie-Qiang (江铁强), Chen Li-Jie (陈立杰), Zhao Yang (赵阳)
Chin. Phys. B, 2014, 23 (**6**): 064702. DOI: 10.1088/1674-1056/23/6/064702

Experimental study on characteristics of isopropanol ejection driven by electrohydrodynamics

Xi-Hao Zhang(张玺皓)[1,3], Wen-Hua Wang (王文华)[1], Cheng-Nan He(何承南)[1], Yi-Chi Yao(姚奕弛)[1], Bo-Yu Wang (王博宇)[1], Xue-Hong Li(李学红)[2], Zhi-Jian Wang(王智健)[1], Chen Qiu(邱晨)[1], Hai-Yi Sun(孙海轶)[2], Yu-Xin Leng(冷雨欣)[2,†], and Gang Xin(新刚)[1,‡]

[1] *Department of Advanced Optical and Microelectronic Equipment, Shanghai Institute of Optics and Fine Mechanics, Chinese Academy of Sciences, Shanghai* 201800, *China*

[2] *State Key Laboratory of Ultra-intense Laser Science and Technology, Shanghai Institute of Optics and Fine Mechanics, Chinese Academy of Sciences, Shanghai* 201800, *China*

[3] *Hangzhou Institute for Advanced Study, University of Chinese Academy of Sciences, Hangzhou* 310024, *China*

(Received 31 March 2025; revised manuscript received 14 May 2025; accepted manuscript online 22 May 2025)

A droplet generator is one of a key module for realizing the Sn-LPP EUV light source. One way of improving a conversion efficiency (CE) and relax tin contamination issue of Sn-LPP EUV light source is to produce tin droplet targets with suitable size. Less than several 10-μm nozzles are used to generate tin droplets. Particles from environment and chemical reaction compounds with high temperature tin cause nozzle clogging issue often. It is significant to develop a technical approach using a large diameter nozzle to produce mass-limited targets. Therefore, this paper demonstrated droplet ejection experiments based on electrohydrodynamics (EHD). Characteristics of isopropanol (IPA) droplet ejection by EHD droplet production platform that was designed and constructed in our laboratory. Characteristics of various process parameters on the IPA droplet production process were investigated. Images of droplet formation process were observed by using a droplet observation system and analyzed by image analysis software. Consequently, the smallest IPA droplet with a diameter of 13 μm could be produced using a nozzle with a diameter of 50 μm. Additionally, the EHD method could make droplets from 13 μm to 55 μm with applying voltage from 5.5 kV to 2.5 kV. In the future, EHD will apply to make mass-limited tin droplet targets under vacuum and high-temperature conditions, in order to increase the CE and to decrease tin debris.

Keywords: EUV light source, electrohydrodynamics, droplet generation, isopropanol

PACS: 47.20.Dr, 47.55.db, 47.55.nb, 47.65.–d

DOI: 10.1088/1674-1056/addbcc **CSTR:** 32038.14.CPB.addbcc

1. Introduction

In recent years, China has achieved a few innovations in the fields of integrated circuits,[1] artificial intelligence,[2,3] cloud computing,[4] new energy vehicles,[5,6] etc. China continues to cultivate deeply development of future industries such as quantum technology,[7] embodied intelligence and 6G,[8–10] etc. As a result, the demand in China for high-performance chips is rising yearly, and the production of high-end chips relies heavily on extreme ultraviolet lithography (EUVL) technology. With the continuous development of EUVL, the semiconductor advanced process has been pushed to 2-nm node and below nodes.

Sn-LPP EUV has become the mainstream EUVL light source solution after 20 years of technology development, with using a high-power laser to shoot on tin droplet targets to obtain high-density and high-temperature plasma that emits EUV light to outside.[11,12] A conversion efficiency (CE) of tin plasma in the process of EUV radiation is affected by many factors, size of tin droplet target, pre-pulse laser, and main pulse laser. In order to obtain a maximum CE of EUV, it is necessary to investigate an optimal laser condition and debris mitigation conditions during the plasma formation and EUV light emission process.[13] However, such applications request to produce a suitable size of tin droplet targets. As a result, the droplet generator is one of key modules for EUV light source. Its performance effects on a CE of the EUV light and the lifetime of EUV collector and light source output.

Currently, many researchers have developed and investigated the topic in China. Huazhong University of Science and Technology conducted a series of droplet injection experiments around the development of the droplet generator. They were able to produce and generate 187-μm tin droplets at a frequency of 25 kHz.[14] The scientists in Shanghai Institute of Optics and Mechanics of the Chinese Academy of Sciences developed a high repetition frequency continuous tin droplet target generator, which is capable of producing uniform tin droplet arrays of 40 μm with a space of 230 μm at a frequency of 100 kHz.[15] All of the above droplet generators were developed based on the Rayleigh jet fracture theory to achieve continuous and uniform droplet production.

†Corresponding author. E-mail: lengyuxin@mail.siom.ac.cn

‡Corresponding author. E-mail: xingang@siom.ac.cn

© 2025 Chinese Physical Society and IOP Publishing Ltd. All rights, including for text and data mining, AI training, and similar technologies, are reserved.

A liquid tin stored in the high-temperature tank is ejected from a nozzle orifice by applying background gas pressure. In addition, a jet stream is also perturbed at a specific frequency by a piezoelectric transducer (PZT), causing it to break up into equal-sized, uniformly spaced droplets. This type of continuous droplet generation technology is essentially an active pressure-based droplet generator. A nozzle diameter limits the produced droplets size. However, smaller nozzles are much more expensive and difficult to produce. Liquid tin becomes very chemically reactive at high temperatures. It can easily form tin dioxide particles with residual oxygen in the chamber. Chemical reaction with tin liquid and storage chamber wall caused clogging of nozzles. Therefore, there is an urgent requirement to develop a droplet generator that can produce small-sized tin droplet targets using a larger nozzle.

Due to the physicochemical properties of tin liquid, small-sized tin droplets must be produced under high vacuum and high temperatures. It is difficult to directly produce tin droplets with a diameter of less than 30 μm due to nozzle clogging problem. Therefore, the first step is to carry out a proof-of-principle method for a production of small droplets with IPA. Physical parameters (i.e., density, viscosity, surface tension, conductivity, and melting point) of liquid material IPA used for the test and tin with a purity of 99.999% are listed in Table 1. The viscosity of IPA is comparable to that of liquid tin. Besides, some studies show that the effect of surface tension and density will result in high-temperature molten metallic tin with both greater surface tension and density exhibiting similar ejection fracture behavior as IPA solutions.[18] Therefore, IPA is valuable to research for characteristics of droplet ejection driven by an EHD method and used to produce 10 μm–30 μm droplets at atmospheric pressure and room temperature.

Table 1. The physics characteristic of IPA and Tin.[16,17]

Physical parameter	Unit	IPA	Tin
Density	kg/m^3	785.5	7280
Viscosity	Pa·s	0.0024	0.0018
Surface tension	N/m	0.0226	0.546
Conductivity	S/m	3.51×10^{-6}	2.9×10^{6}
Melting point	°C	–89	231.9

A method based on the EHD method for producing an ejection of liquid droplets has been widely investigated.[19–21] This method has the capacity to yield a variety of jetting modes and can be employed for either continuous or on-demand preparation.[22,23] Researchers have utilized the EHD method to study conductive polymer deposition,[24,25] three-dimensional (3D) printing,[26] production of micro droplets.

2. Analytical model

2.1. Principle of EHD

A conceptual schematic of the EHD liquid droplet generator and the force balance within a system is shown in Fig. 1, with a set-up in which droplet charging is employed. An electric field-induced liquid ejection is mainly influenced by capillary force, viscous force, surface tension, gravity, and electric force. Besides, the working parameters of an experiment, such as pneumatic pressure, applied voltage, and anode geometry, also influence the behavior of hydrodynamics.[22,27–29] Under EHD conditions, the liquid material converging at a nozzle orifice is exposed to an external electric field. Several charges affected by the electric field accumulate on the surface of a liquid material. Finally, an ejection occurs due to the Coulombic repulsion of the charges overcoming the surface tension. An anode charges a liquid by creating an inductive electric field. This way ensures that a liquid material and an experimental system device are grounded, which greatly improves the safety performance of the system.[30,31] Furthermore, this equipment is designed to produce tin droplets in the future, so a tank needs heaters to work at high temperatures to acquire molten tin. To protect heaters from high-voltage damage, a nozzle and a tank need to be connected to the ground. Therefore, an anode is employed to investigate the characteristics of liquid ejection driven by EHD.

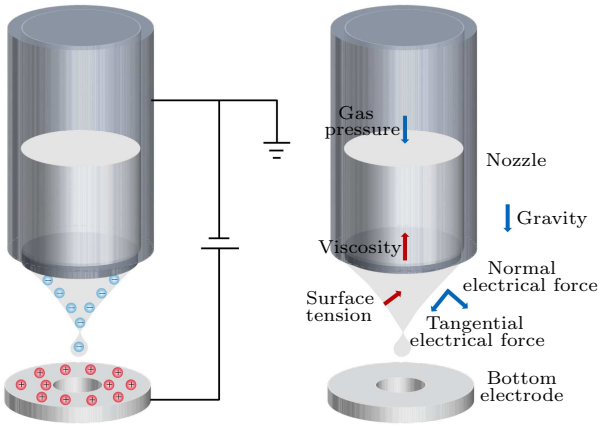


Fig. 1. The principle of the EHD ejection set-ups, including (a) anode, and (b) the force balance between gas pressure, viscosity, surface tension, electrical force, and gravity during EHD ejection.

Under an action of applying an external electric field, a hydrodynamics behavior of liquid is determined by an electric field force, fluid viscous force, and surface tension. In the process of fluid ejection, its corresponding ejection flow rate can be described by Poiseuille's law[31,32]

$$Q=\frac{\pi d_n^4}{128\mu L}\left(\frac{\varepsilon_0 E^2}{2}-\frac{2\gamma}{d_n}+\Delta P\right). \tag{1}$$

From this equation, Q is a flux of ejection flow, d_n is the diameter of meniscus, μ is a viscosity of a liquid material, L is a length of a nozzle, ε_0 is a permittivity of vacuum, E is an intensity of an electrical field, γ is a surface tension regarding an interface between air and liquid material, and ΔP is a pressure drop between an inlet and an outlet of a nozzle by a pressure controller. In summary, $\varepsilon_0 E^2/2$ is an electric pressure, $2\gamma/d_n$ is a capillary pressure, and ΔP is a hydrostatic pressure, which

is used to drive liquid through a thin nozzle. Besides, a value of an electrical force is also influenced by an intensity of an electrical field, and its distribution on an axis of a high-voltage anode can be described as follows:[33,34]

$$\boldsymbol{E} = \frac{4V}{d_n \ln(8h/d_n)}, \tag{2}$$

where V and h are an applied voltage and a working distance between a nozzle and an anode. From this equation, it is known that a jet will be affected by process parameters such as fluid physical parameters, nozzle specifications, applied voltage, and height between a nozzle and an anode, background gas pressure, etc. during an ejection process. However, equation (2) ignored a structure of anode inner diameter based on EHD method. In this work, a hollow anode was adopted to apply high voltage inducing the IPA ejection. Besides, in order to help the IPA droplets through an anode. A center hole was made internally above the anode.

2.2. Distribution of electric field on axis model

According to Eq. (2), the intensity of an electric field ignores the influence of an inner diameter of an anode. In this study, the experimental anode structure is annular and internally hollow. Therefore, it is necessary to establish the electric field distribution model on the axis of an anode. First of all, the model is simplified, assuming that the ring anode is a hollow circle with a radius of r, and there is a point on the axis of the circle with a distance of h from the center of the circle, and then the field strength model of the hollow circle to the point on the axis is shown in Fig. 2.

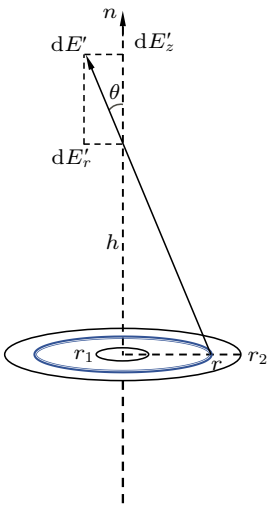


Fig. 2. The schematic diagram of a hollow ring of an electric field intensity on the axis hollow anode.

Intercept a microelement on the hollow rings, the microelement for the point on the axis of the electric field strength according to Coulomb's law,[35] i.e., $\mathrm{d}\boldsymbol{E}' = \mathrm{d}q(4\pi\varepsilon_0 r^2)^{-1}$. According to the symmetry, it is easy to know that the $\mathrm{d}E'_{\boldsymbol{r}}$ component is 0. Thus, the electric intensity of a hollow ring with radius r can be calculated as $\mathrm{d}E\boldsymbol{z}' = hq\boldsymbol{n}[4\pi\varepsilon_0(h^2+r^2)^{1.5}]^{-1}$, where the electric field model on the axis of the ring is established. As shown in Fig. 2, where a hollow ring with inner diameter r_1 and radius r_2, which can be regarded as several hollow rings put together, and take a ring with width $\mathrm{d}r$, especially, $\boldsymbol{n}$ is the vector of z direction. Assuming that its surface charge density is σ_0. Therefore, the charge carried by the micro metabolite can be calculated in the following way, $\mathrm{d}q = \sigma_0 \cdot 2\pi r \mathrm{d}r$. Finally, the electric field intensity of a hollow ring anode on axis can be calculated as integrates $\mathrm{d}E\boldsymbol{z}'$ and $\mathrm{d}r$ successively gives

$$\boldsymbol{E}' = \frac{\sigma_0 h\boldsymbol{n}}{2\varepsilon_0}\left(\frac{1}{\sqrt{h^2+r_1^2}} - \frac{1}{\sqrt{h^2+r_2^2}}\right). \tag{3}$$

According to a field strength distribution relationship on an anode axis, it can be obtained that changing a distance between a nozzle and an anode affects and changes an electric field strength of a liquid surface at a nozzle. In order to study an effect between changing a working distance and an inner diameter of an anode on the droplet and production process, it is necessary to ensure that a magnitude of a field strength applied to a liquid surface of a nozzle at different working distances or different inner diameters are unchanged. In this model, the model was considered as a capacitor. Therefore, the number of charges can be calculated as $Q = CV$, $C = \varepsilon A(h)^{-1}$, where C, Q, A, ε are capacitance, charge, area of an anode, respectively; and ε is permittivity of air.

According to Poiseuille's law, the achievement of droplet ejection driven by EHD method on the premise that the electric field force overcomes the effect of surface tension can be described as follows: $0.5\varepsilon_0 \boldsymbol{E}'^2 = 2\gamma(d_n)^{-1}$. Finally, a simple analytic model that represented an electric field distribution on the axis of a conical anode was constructed.

3. Experimental set-ups

This paper is based on the EHD method to study the production of tiny droplets. IPA droplet ejection test was carried out with a platform at room temperature and normal pressure driven by EHD method. Schematic drawing of platform is shown in Fig. 3. IPA droplet production experiment under constant voltage was carried out.

A key part of the EHD droplet production platform is the high-voltage anode droplet generation unit. The anode is connected to the positive pole of the high-voltage power supply, and the liquid storage chamber and nozzles are grounded. By forming an induced electric field between the nozzle and the anode, droplets are generated from a liquid jet. It is worth to be mentioned that a nozzle of a droplet generation unit is a capillary glass nozzle (orifice diameter of 50 μm, nozzle cross-section diameter of 35 μm), as shown in Fig. 4. IPA

was installed in a liquid storage chamber of a droplet generator, and a chamber was connected to compressed argon gas through a pipeline. When a value of background gas pressure was low, liquid was easily covered at a nozzle cross-section due to surface tension.

Besides, a compressed argon gas was input to the pressure controller after pressure was reduced to approximately 4 bar (1 bar = 10^5 Pa) via a pressure-reducing valve. The computer was utilized to operate the pressure controller. It controlled a background gas pressure in the range of 0–200 mbar to the IPA storage tank, which is used to drive IPA liquid to reach a nozzle orifice to realize a passive liquid supply. By controlling an output pressure, it is possible to change a flow rate of a liquid supply or to maintain a curved liquid level near a nozzle orifice. Besides, a signal generator (AFG31022, Tektronix Inc.) was used to generate required high-voltage waveforms, which were passed through a high-voltage amplifier (2290-10, Keithley Inc.) and output to a pulsed signal controller (PVX-4130, BNC Inc.), which outputs high voltage pulse or DC voltage. A high voltage probe (P6015A, Tektronix Inc.) is used to monitor real-time voltage waveforms.

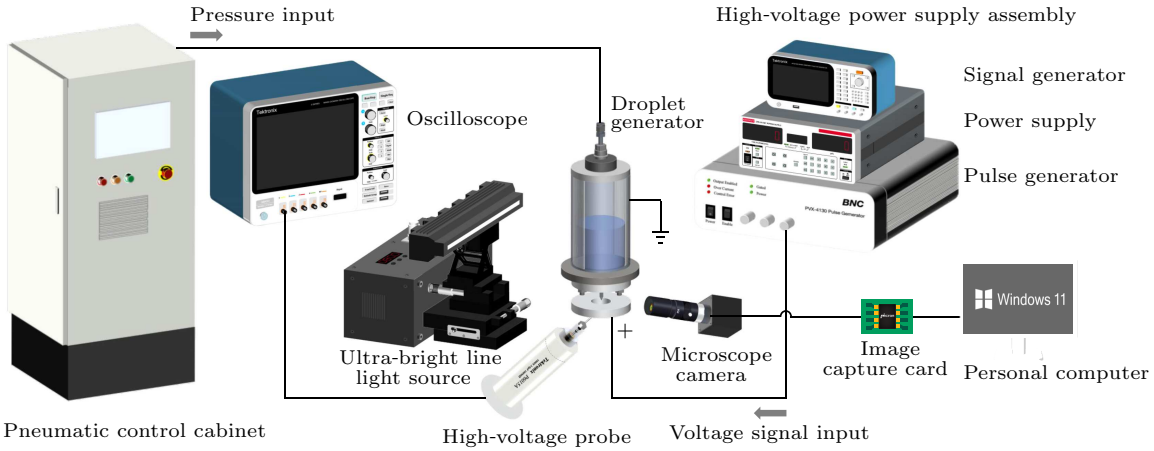


Fig. 3. Schematic drawing of an atmospheric EHD platform includes a droplet generator, an anode, a pneumatic control cabinet with Ar gas supply, a high-voltage power supply assembly (which consisted of a signal generator, a power supply, and a pulsed generator), a microscope camera, an ultra-bright line light source, an image capture card, and a personal computer.

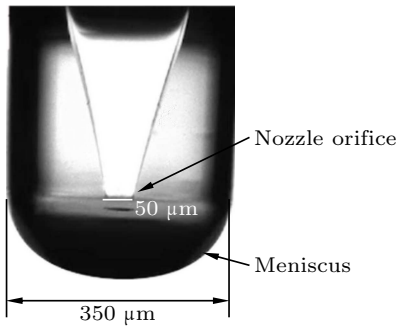


Fig. 4. The structure of a nozzle whose orifice diameter is 50 μm and cross-section diameter is 350 μm.

The metrology system of atmospheric pressure and a room temperature EHD droplet generation platform used a shadow imaging method to observe IPA jet and droplets formation process. As shown in Fig. 3, the metrology system uses a COMS camera (MV-CH089-10UM, Hikvision Inc.) with an exposure time of 1 μs and pixels of 3.45 μm, and a high-resolution non-coaxial telecentric lens with a working distance of 65 mm for the camera's microscope head (MH65201B, Chiopt Inc.). A light source was an ultra-bright line light source (LTS-4LINH300-R/BGW-252W, Lots Inc.). After a camera completed raw images acquisition, an image processing software was used to obtain diameters and coordinate information of droplets.

4. Results and discussion

As shown in Fig. 5, based on an EHD method, IPA droplets could be produced and ejected from a nozzle orifice by an external electric field. An ejection mode was changed under different applied voltages. A few droplets formed by applying a constant high pressure between an anode and a nozzle to produce a cone-jetting mode were relatively stable in size. Furthermore, a jet at the bottom broke into smaller droplets due to the Rayleigh instability.[36] Therefore, a microdroplet production method based on a stable cone-jetting mode provides a more reliable method and technology for the production of stable-sized molten tin droplets. In order to produce a mass-limited tin target in the future, based on the current experimental system, effects of different process parameters on a stable generation of cone-jetting will be investigated. When a background gas pressure, an anode working distance, and other working conditions remain constant, the electric field intensity between a nozzle and an anode was modulated by adjusting a voltage output value of the high-voltage power supply. When an applied electric field intensity achieves sufficient criteria, an electric field force and a gas pressure are adequate to overcome a surface tension of liquid material and maintain a stable cone-jetting. Finally, a voltage value corresponding to this electric field intensity is determined as a voltage threshold.

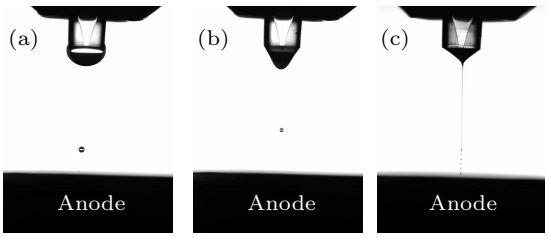


Fig. 5. Droplets formation modes with different externally applied voltages at a fixed working distance of 1.3 mm, inner diameter of 3 mm, and background gas pressure of 1.0 mbar. (a) Dripping mode, applied voltage range from 2 kV to 3 kV; (b) micro-dripping mode, applied voltage range from 3.5 kV to 4.5 kV; and (c) cone-jetting mode, applied voltage range from 5.2 kV to 6 kV.

4.1. Influence of high-voltage on formation of droplets

4.1.1. Image processing to observe droplet generation

A software of measurement of droplets was developed to obtain images of droplet production process, as shown in Fig. 6. Magnification and pixel size were input into an image analysis software to determine droplet sizes and spatial positions. The image analysis software used a smoothing algorithm to process from original droplet images, which firstly used the Gaussian smoothing filtering algorithm for noise reduction. Software binarized the images and finally used the gradient Hough algorithm to identify droplet contours and then drew a circle on the original images. At the same time, it output information such as center and diameter of droplets. As shown in right side of image in Fig. 6. Droplets with a diameter of 13 μm were produced using a nozzle with a diameter of 50 μm, and the interval of two droplets was approximately 40 μm.

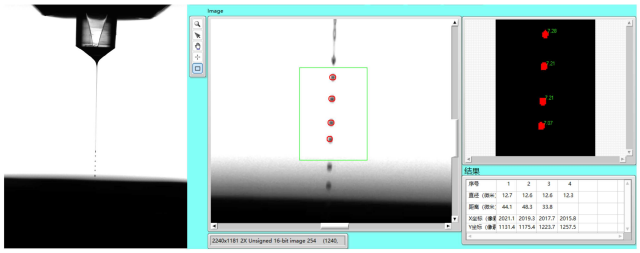


Fig. 6. Software and analyzed IPA droplets.

To evaluate the stability of the droplet size generated by an EHD method, the fabrication process of droplets over a long time was recorded by a camera. A total recording duration of approximately one hour was achieved through intermittent video acquisition for 10 s recordings captured with 5-min intervals. Each video file was divided into 215 frames. For each figure, droplets was 4 in each image, as shown in Fig. 6. The horizontal axis in Fig. 7(b) corresponds to the number of sequences from 1 to 4 for each sampled droplet, with different ordinal numbers representing droplets at different locations. The results of the droplet diameter obtained were shown in Fig. 7(a). After analysis and calculation, the range of droplet diameter was from 11 μm to 15 μm, and the droplet diameter standard variance was around 1.4 μm. The error may come from an experimental condition setting, a Rayleigh instability, or a software process.

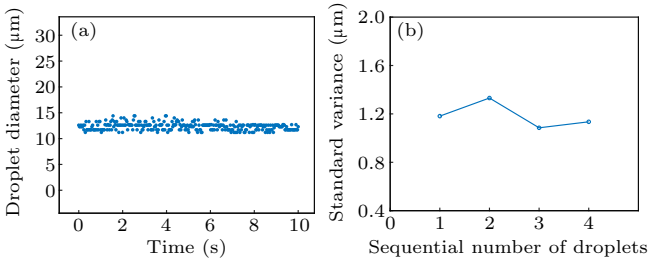


Fig. 7. (a) The plot of droplet diameter for 10 seconds taken with an inner diameter of 3-mm anode and with a working distance of 1.3 mm with applied voltage 5500-V DC and background gas pressure of 1.0 mbar. (b) Standard deviation of droplet diameters of 10 seconds.

4.1.2. Effects of applied voltage on droplet diameters

In a process of generating liquid droplets by jet ejection are as following, a curved liquid surface was formed, and then injected by injection, contraction, and fracture under the action of electric field force to form liquid droplets. The core of the liquid to produce jets is the electric field force and the liquid surface tension together. When an applied voltage was too low, the electric field intensity was not enough to drive the liquid deformation to produce a cone-jetting, the curved liquid surface will oscillate under the action of the electric field force. When an applied voltage was too high, it may lead to the atomization of the bottom end of the jet or the generation of multi-jet modes. In the study of the effect of voltage on the droplet production process, other working conditions were kept constant, and when the background gas pressure was 1.0 mbar, the inner diameter of the anode was 3 mm, the working distance of the anode was 1.3 mm, and the diameter of the curved liquid surface was around 350 μm, the droplet jets under the effect of different voltages are shown in Fig. 8.

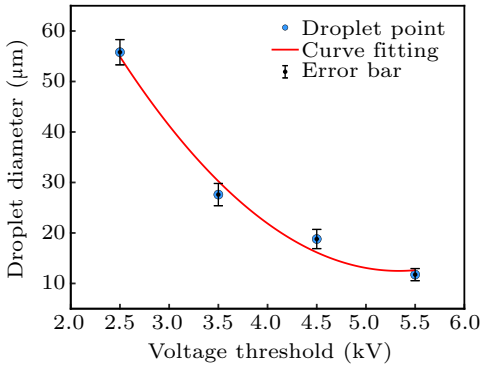


Fig. 8. Relationship between droplet diameters and applied voltages on the anode, at a fixed anode of inner diameter 3 mm and working distance 1.3 mm under background gas pressure 1.0 mbar.

Dripping mode occurs under lower voltage conditions less than 3 kV and background gas pressure with 1.0 mbar, due to field force has less influence on the whole droplet production process, so surface tension and gravity forces dominate. As the voltage raised to 5.5 kV, the electric field was gradually enhanced, and the liquid surface deformed under the

action of the electric field, such as Fig. 5(c), where the liquid surface at the nozzle forms a Taylor cone, and since the electric field force was not enough to maintain a stable cone-jetting, the liquid surface was quickly deformed and contraction phase and break to produce small droplets. Diameter of the droplets produced by this mode was smaller than that of the dripping mode. With voltage continuously increased, the strong electric field eventually drove a liquid surface to form a Taylor cone similar to a microdroplet mode, except that a tip of the Taylor cone produced a continuous stream of elongated jets. At the same time, the bottom of the cone-jetting will continue to fracture to produce droplets due to the Rayleigh instability. Among them, the results of droplet diameter variation with voltage are shown in Fig. 8. It is easily seen that the production of droplets of different sizes can be achieved by changing the voltage, and different microdroplet production modes have been realized, including dripping mode producing droplets around 55 μm, micro-dripping mode producing droplets around 20 μm, and cone-jetting mode producing droplets around 13 μm.

4.2. Influence of background gas pressure on threshold voltages to generate droplets.

Correlation between background gas pressure and threshold voltage was investigated and shown in Fig. 9. When an inner diameter of an anode was 3 mm, a distance between an anode and a nozzle was 1.3 mm, and a diameter of a liquid meniscus was 350 μm. An experimental result showed that to drive the liquid through a thin nozzle to an orifice to maintain a meniscus, a background gas pressure of at least 0.4 mbar was required. Therefore, a pressure controller was used to inject a compressed gas in the range of 0.4 mbar–2 mbar into the chamber, with a single change of 0.1 mbar. Meanwhile, 5 V per 0.1 mbar increases in voltage. It was found that under constant DC voltage conditions when the gas pressure was 0.4 mbar, the voltage threshold for maintaining a stable cone-jetting was 5300 V. Furthermore, gradually increasing a voltage resulted in a jet returning to stable cone-jetting mode.

As a gas pressure gradually increased from 0.4 mbar to 1.9 mbar, voltage thresholds required to sustain a stable cone-jetting mode also rose from 5300 V to 5450 V, exhibiting an increased rate of 100 V/mbar. It should be known that the background gas pressure required to drive IPA arriving at a nozzle orifice was constant. It was evident that an increase in background gas pressure would result in a greater volume of IPA expelled from a nozzle due to a surplus of pressure. It leads to more liquid accumulation at a nozzle orifice. The necessity for a greater electrical force to overcome surface tension was thus established to maintain a stable cone-jetting mode. In summary, the electric field force required to maintain a stable cone-jetting increased with more liquid supply. And the voltage thresholds rose up with increasing background gas pressures.

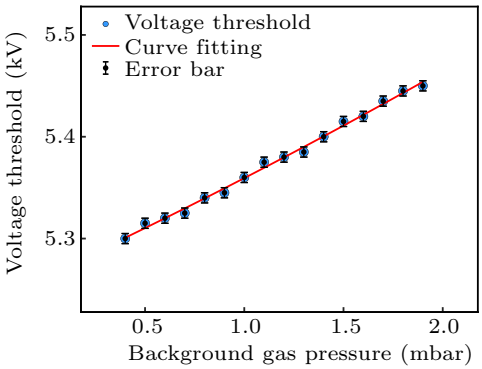


Fig. 9. Voltage thresholds required to maintain a stable cone-jetting under different background gas pressures at a fixed anode of inner diameter 3 mm and working distance 1.3 mm.

4.3. Influence of high-voltage anode on formation of droplets

4.3.1. Effect of an anode working distance *versus* voltage thresholds

During this experiment, an anode with an inner diameter of 3 mm was used. When the anode working distances h of 0.8 mm, 1.3 mm, and 1.8 mm, the background gas pressure and applied voltage conditions required to maintain a stable cone-jetting at the corresponding working distances were recorded, as shown in Fig. 10. It can be seen that the voltage threshold increased with increasing anode working distances.

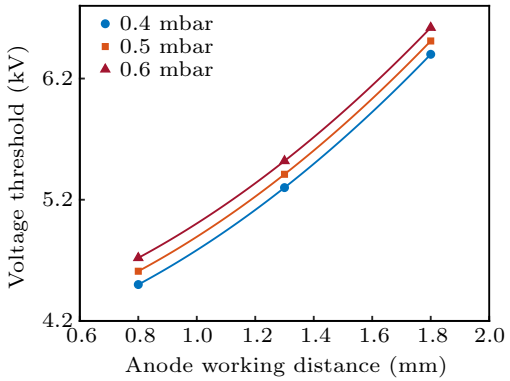


Fig. 10. Correlation between voltage thresholds and anode working distance to maintain a stable cone-jetting. Experiments had been done with a 3-mm hollow anode. Working distances of 0.8 mm, 1.3 mm, and 1.8 mm. Background gas pressures of 0.4 mbar, 0.5 mbar, and 0.6 mbar.

According to the on-axis field strength distribution relationship Eq. (2), it is easy to know that the field intensity decreases with increasing working distance of an anode when an applied voltage and liquid surface diameter at a tip of nozzle are kept constant, then the electric force acting on the surface of the fluid decreased gradually with increasing working distance. However, an electric force to maintain the stabilized cone-jetting was not changed. Hence, it is necessary to increase the electric field intensity by increasing the voltage to

maintain the stable ejection of the jet, as shown in Fig. 10. Increasing the working distance of the anode will increase the voltage threshold required to maintain the stabilized cone-jetting. Finally, the equilibrium in the ejection process was easily influenced by working parameters, so it must pay more attention to controlling the modification of these parameters.

4.3.2. Effect of hollow anode inner diameters *versus* voltage thresholds

Tapered hollow anodes with inner diameters of 1 mm, 3 mm, and 5 mm were used in the experiments to study effect of an inner diameter of anodes on droplet generation process. As shown in Fig. 11, when a background gas pressure, liquid surface diameter at the tip of a nozzle, and other working conditions remained constant, with increasing inner diameter of an anode, the voltage required to maintain a stable cone-jetting gradually increased. According to Eq. (3), a value of an electric field intensity decreased with an inner radius of an anode, which led to an electric force decreasing and not being enough to overcome a fixed surface tension. Therefore, the value of a voltage needed to be increased to create a larger external electric field intensity.

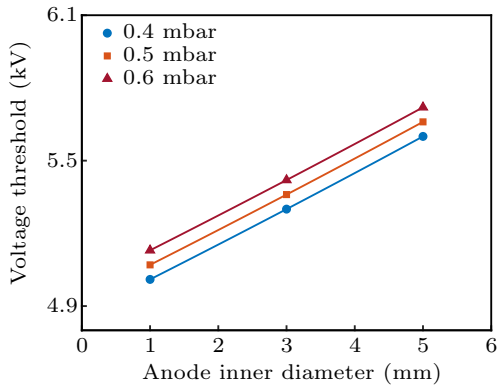


Fig. 11. Plots of voltage thresholds were required for an anode to maintain a stable cone-jetting at a fixed working distance of $h = 1.3$ mm and different inner diameters (1/3/5 mm) at corresponding gas pressures (0.4/0.5/0.6 mbar).

In summary, the change in an inner hollow diameter of anode affected the electric field distribution, which affected force balances between a background gas pressure force, an electric force, a liquid gravity force, viscosity force, and surface tension, leading to a change in the voltage threshold required to maintain a stable cone-jetting.

4.4. Future challenges

This study successfully demonstrates the feasibility of an EHD approach for generating small-sized IPA droplets using enlarged nozzles. However, extending this methodology to tin droplet generation for an application of EUV light source requires overcoming key challenges specific to molten tin. The primary issue in preparing liquid tin is high chemical reactivity at high temperatures.

Liquid tin is easily oxidized in the presence of oxygen,[37] forming tin dioxide (SnO_2) at a tip of a nozzle, which leads to nozzle clogging. Besides, particles from a clean room, poor purity of tin material, and other impurities from a droplet generator wall cause clogging issues.[14] To mitigate the problem, a droplet generation process needs to be done in a high vacuum and a clean environment. In addition, the nozzle geometry will be optimized to avoid a nozzle cross-section being completely covered due to surface tension of liquid tin.

5. Summary

In this paper, we made an EHD droplet injection platform for a production of small IPA droplets less than 30 μm at room temperature. A model of an electric field intensity distribution on the axis of an anode and experimental results were compared and discussed. The effects of different process parameters and geometry of electrical field on the droplet production process were analyzed experimentally. Three droplet generation modes of droplets were realized based on the EHD method with varying back pressure and varying electric field. They are (i) dripping mode, (ii) micro-dripping mode, and (iii) steady cone-jetting modes.

As a consequence, following characteristics of a steady cone-jetting were obtained as follows. (I) A voltage threshold to generate IPA droplets was increased with a working distance of anodes, with an increase of background gas pressure with a rate of 10 V/mbar. (II) In addition, a voltage threshold was increased due to an increase inner diameter of an anode. It decreased electric field strength around IPA, while an electric force required to maintain a stable cone-jetting remains constant. Therefore, it needs to increase an applied voltage to provide sufficient electric field intensity to form bigger electric force.

Diameter of produced droplets decreased with increasing voltage applied to an anode. IPA droplets with a diameter from 13 μm to 55 μm were obtained with applying voltage from 5.5 kV to 2.5 kV. The smallest IPA droplet size was achieved at around 13 μm with using a nozzle with a diameter of 50 μm. In the future, tin droplets with less than 30 μm will be produced under high-temperature vacuum conditions based on the EHD method. Small tin droplets can be used to study plasma physics-related EUV light sources.

Acknowledgement

Project supported by the Strategic Priority Research Program of the Chinese Academy of Sciences (Grant Nos. XDA 0380000 and 0380300).

References

[1] Harjani M 2024 *Asia Policy* **19** 51
[2] Ebert C and Wang X Y 2024 *Computer* **57** 97
[3] Zhou Y, Yan L and Liu X 2024 *Journal of Data and Information Science* **9** 155
[4] Xia Y 2024 *Science China Information Sciences* **67** 1
[5] Kendall and Michaela 2018 *Progress in Natural Science: Materials International* **28** 113
[6] Kimble C and Wang H 2013 *Journal of Business Strategy* **34** 13
[7] Zhang Q, Xu F H, Li L, Liu N L and Pan J W 2019 *Quantum Science and Technology* **4** 040503
[8] He Z, Huang H, Zhang P, Ma D R, Shi B H, Wang T, Huang Y Y and Guo J 2024 *Chin. Opt. Lett.* **23** 110603
[9] Wang G Y, Bao H N, Liu Q, Zhou T G, Wu S, Huang T J, Yu Z F, Lu C W, Gong Y H, Zhang Z X and He S 2024 *Science China- Technological Sciences* **67** 2282
[10] Wu C W, Yue X, Shu F and Wu G 2024 *China Communications* **21** 69
[11] Zong N, Hu W M, Wang Z M, Wang X J, Zhang S J, Bo Y, Peng Q J and Xu Z Y 2020 *Chin. Opt.* **13** (in Chinese)
[12] Lin N, Yang W H, Chen Y Y, Wei X, Wang C, Zhao J L, Peng Y J, and Leng Y X 2022 *Laser & Optoelectronics Progress* **59** 20 (in Chinese)
[13] Gao C, Liu Y P, Yan G P, Yan J, Chen X Q, Hou Y, Jin F T, Wu J H, Zeng J L and Yuan J M 2023 *Acta Phys. Sin.* **72** 183101 (in Chinese)
[14] Chen H 2015 *Characterisation of laser plasma debris and extreme ultraviolet radiation from droplet tin targets* Ph.D. Dissertation (Wuhan: Huazhong University of Science and Technology) (in Chinese)
[15] Sun H Y, Wang G D, Li X H, Peng K L, Zou J J, Peng Y J, Wang C, Leng Y X, Xu J H, Fan L L, Yuan F H, Li Z L, Bu Y, Wang T Z, Zhang Z Y, Xin G and Lin N 2023 *Laser & Optoelectronics Progress* **60** (in Chinese)
[16] Grigoryev S Y, Dyachkov S A, Khokhlov V A, Zhakhovsky V V and Inogamov N A 2019 *J. Phys. Conf. Ser.* **1147** 012067
[17] Jolliff H A and Isopropyl Alcohol 2016 *Critical Care Toxicology*
[18] Zou K 2024 *The Preparation, Performance and Application Study of Piezoelectric High-Temperature Tin Droplet Generator for EUV Photolithography Light Source* Ph.D. Dissertation (University of Chinese Academy of Sciences) (in Chinese)
[19] Wei C, Gang T Q, Chen L J and Zhao Y 2014 *Chin. Phys. B* **23** 064702
[20] Fylladitakis E D, Theodoridis M P and Moronis A X 2014 *IEEE Transactions on Plasma Science* **42** 358
[21] Jiang H Y, Ren Y K, Ao H R and Romans A 2008 *Chin. Phys. B* **17** 4541
[22] Mishra S, Barton K L, Alleyne A G, *et al*. 2010 *Journal of Micromechanics & Microengineering* **20** 095026
[23] Porter B F, Mkhize N and Bhaskaran H 2017 *Microsystems & Nanoengineering* **3** 9
[24] Han Y and Dong J 2018 *Advanced Materials Technologies* **3** 1700268
[25] Xu L, Wang X, Lei T P, Sun D H and Lin L W 2011 *Langmuir the Acs Journal of Surfaces & Colloids* **27** 6541
[26] Wang K and Stark R P W 2010 *Appl. Phys. A* **99** 763
[27] Back S Y, Song C H, Yu S, Lee H J, Kim B S, Yang N H, Jeong S H and Ahn H 2012 *Journal of Nanoscience and Nanotechnology* **12** 446
[28] Kim D S, Khan A, Rahman K, Khan S, Kim H C and Choi K H 2011 *Advanced Manufacturing Processes* **26** 1196
[29] Lee M W, Kim N Y and Yoon S S 2013 *Journal of Aerosol Science* **57** 114
[30] Mkhize N and Bhaskaran H 2022 *Small Science* **2** 1
[31] Xu C X, Huang Y, Fu J Z and Markwald Roger R 2014 *Journal of Micromechanics & Microengineering* **24** 115011
[32] Chen C H, Saville D A and Aksay I A 2006 *Appl. Phys. Lett.* **89** 1842
[33] Eyring C F, Mackeown S S and Millikan R A 1928 *Phys. Rev.* **31** 900
[34] Marginean I, Netnes P and Vertes A 2006 *Phys. Rev. Lett.* **97** 064502
[35] Ivchenko V 2021 *European Journal of Physics* **42** 065201
[36] Sharp D H 1984 *Physica D* **12** 3
[37] Li J, Yuan Z F, Qiao Z Y, Fan J F, Xu Y K and Ke J J 2006 *Journal of the Chinese Rare Earth Socirty* **24** 190 (in Chinese)